Stacked analysis of earthquake sequences: statistical space-time definition of clustering and Omori law behavior

Tosi P.(1), De Rubeis V.(1) and Sbarra P.(1)

(1) Istituto Nazionale di Geofisica e Vulcanologia, Roma, Italy.

Abstract

The definition of the aftershocks sequence is still a debated topic. We here propose a study of the spatial and temporal variation of the earthquakes clustering and rate decay. We used five different seismic catalogues, characterized by specific spatial and magnitude ranges. They are respectively: world one, for a global analysis, Greek, Japanese, Californian and Italian regional catalogues in order to investigate different seismo-tectonic settings.
A stacking procedure has been applied to characterize a typical sequence behavior and allowing the evaluation of changes over time intervals (τ) and distances (r) from the main shock. The resulting decay rate $p(r,\tau)$ has values comparable to the modified Omori law: $p(r,\tau) \simeq 1$ at small distances and inside specific time ranges. It is then possible to define sequences into a particular spatial range varying in time and reaching a maximum distance of 50-100 *km*. In a first time period (until 10-20 days) the slope p is small before reaching the typical sequence value ($p \simeq 1$). The slope of the first period increases with increasing threshold magnitude. This dynamics highlights the importance of looking at proper space-time limits when analyzing the seismic decay after a main shock. Different decay domains have been evidenced: they depend on the threshold magnitude of the catalog and are characterized by smooth variations in space.
Catalogues have been analyzed under the fractal dimension aspect as related to the space and time clustering. Even in this case a pattern behavior of seismicity has been evidenced. After the occurrence of an event there is a space-time domain inside which the subsequent events are temporally related. Inside this domain the seismic sequences drive temporal occurrences. Concerning the space correlation dimension, results reveal the presence of a space clustering of hypocenters for distances greater than few tenth of *km* and for time intervals less than hundreds of days. At short distances hypocenters are time clustered but there is not space clustering. This zone is probably due by the activity of seismicity on the seismic fault.
Relations between decay rate domains and clustering domains in space and time are evidenced and discussed.

Introduction

Earthquakes are the answer to tectonic load; stress is redistributed through the earthquakes, causing the aftershock sequence to develop in space and in time. Triggering of earthquakes may acts at several spatial and time scales. Short-range triggering (distance of the order of seismic fault size) is due by stress changes induced by the main-shock and related aftershocks in a recursive process.
Long-range triggering is a more difficult aspect to explain. Experimental evidences as well as physical explanations or synthetic earthquakes generation were proposed. They include analysis for geothermal sites, Coulomb-stress modifications, the application of declustering algorithms, multiple stress transfer, cellular automata behavior and the consideration that the crust is in a critical state (Tosi et al, 2008; Hill et al., 1993; Husen et al., 2004; Brodsky et al., 2000; Godano et al., 1999; King et al., 1994; Stein et al., 1994; Stein, 1999, Melini et al., 2002; Marzocchi et al., 2003; Ziv,

2006; Bak and Tang, 1989). Other authors have attempted to find space-time relations of seismicity in order to study long-range relations for both global and regional catalogues.
Influence ranges of the order of 100 km from main shocks were recognized (e.g., Gasperini and Mulargia, 1989; Reasenberg, 1999). For highest magnitude earthquakes of last century, Lomnitz (1996) found very long-range correlation. Marsan et al. (2000) investigated space-time relations of scale-invariance of seismicity. They pointed out that space and time should not be considered separately, but rather the spatial correlation structure is evolving in time. They considered migration of aftershocks away from the main shock in a form of a sub-diffusive process.
Several questions arise from the complexity of results and interpretations. Long range triggering is to be considered rare and peculiar to specific situations? Is the sequence extension in space constant, with the same parameters of the Omori law? Is a sequence the result of multiple overlapping Omori functions with shifted starting time, produced by remarkable aftershocks, as suggested in Ogata et al. (2003)? Does aftershock duration scale with the mainshock size? Ziv (2006) posed the question and found no correlation with magnitude of main. What is the origin of c Omori parameter? Is it physical or due to catalogue incompleteness? What is the role of static and dynamic stress triggering?
To address these questions it is important to consider the spatial and temporal aspects of the seismic process simultaneously, in a combined way. In this work we apply a method of analysis (Tosi et al., 2008), suitable to point processes and based on space-time correlations among earthquakes. Like the previously cited authors, we do not separate seismicity into main and aftershocks.

Data

A set of seismic catalogues has been chosen, covering different space and time ranges. Although there is strong scale invariance in seismic activities, geophysical constrains are present like crustal thickness and the dimension of plate boundaries, as well as instrumental limits like time length of dense seismic station networks, completeness of recordings etc..
In total five different seismic catalogues have been analyzed. They have been firstly investigated on their completeness. A reliable method to assess completeness magnitude threshold is based on the application of the Gutenberg-Richter (GR) law to magnitude distribution. It is given by: $\log N = a - bM$, where N is the cumulative number of events with magnitude bigger or equal to M , a and b are constant. Coefficient a is related to the seismic activity level, while b is a quite robust parameter with values near 1. Assuming the validity of this law, a clear anomaly of the distribution at lower magnitudes may indicate a lack of completeness in the selected time range. After cutting earthquakes below the threshold magnitude and for depth greater then 50 km, resulting catalogues are here summarized (figure1).

- Global CMT catalogue (Centroid Moment Tensor, Harvard). It covers a time span from January 1980 to December 2004, threshold magnitude of completeness is 5.5 and maximum recorded magnitude is 9.5. The number of events is 13268.
- Greece catalogue (Geophysical Laboratory, University of Thessaloniki). It covers a time span from January 1964 to September 2007, threshold magnitude of completeness is 4.5 and maximum-recorded magnitude is 7.5. The number of events is 5865.
- Japan catalogue (selection of USGS NEIC catalogue). It covers a time span from January 1980 to October 2008, threshold magnitude of completeness is 4.5 and maximum recorded magnitude is 8.3. The number of events is 6698.
- South California catalogue (Southern California Earthquake Center, relocated by Shearer et al., 2005). It covers a time span from January 1984 to December 2002, threshold magnitude of completeness is 2.0, but for this analysis we cut the catalogue at 2.5. Maximum-recorded magnitude is 7.3. The number of events is 23576.

- Italy catalogue (INGV CSI 1981-2002 and ISIDE 2002-2009). It covers a time span from January 1988 to May 2009, threshold magnitude of completeness is 2.0, but for this analysis we cut the catalogue at 2.5. Maximum-recorded magnitude is 5.8. The number of events is 11860.

These catalogues represent seismic activity over very different tectonic settings and spatial scales. Global catalogue reflects the activity of the whole planet, focusing to the highest magnitudes events. This catalogue is suitable to study the activities related to high energy stress-strain relation due to global plate tectonics. South California catalogue is a good example of regional transcurrent tectonics seismic activity. Moreover this catalogue derives from a good seismic network, showing a very low completeness magnitude threshold. Among the other regional catalogues, we chose the Italian region, which presents a seismic activity of medium magnitudes, coming from heterogeneous tectonic settings, recorded by a good seismic network too. Greece and Japan catalogues list medium-high magnitudes events; dominating tectonics is plate subduction.

Space-time fractal dimensions of seismicity

The above-described catalogues have been analyzed under their space and time clustering properties through the fractal dimension analysis. We apply the correlation integral method, defined as:

$$C(l) = \frac{2}{N(N-1)} \sum_{i=1}^{N-1} \sum_{j=i+1}^{N} \Theta\left(l - \left\|\mathbf{x}_i - \mathbf{x}_j\right\|\right),$$

where l is the metric of the space considered, N is the total number of elements, $\mathbf{x}$ is the coordinate vector and Θ is the Heaviside step function. If $C(l)$ scales like a power law, $C(l) \propto l^D$, the correlation dimension D can be defined by

$$d(l) = \frac{\delta \log C(l)}{\delta \log l},\ D = \lim_{l \to 0} d(l).$$

Experimentally self-similarity can best be found by plotting the local slope d of $\log C(l)$ versus $\log l$. From this we can extend the correlation integral to a combined space-time approach. It is defined as:

$$C_c(r,\tau) = \frac{2}{N(N-1)} \sum_{i=1}^{N-1} \sum_{j=i+1}^{N} \left(\Theta\left(r - \left\|\mathbf{x}_i - \mathbf{x}_j\right\|\right) \cdot \Theta\left(\tau - \left\|t_i - t_j\right\|\right)\right),$$

where the metrics of space and time are considered simultaneously (Tosi *et al.,* 2008).
Similarly to correlation dimension we define the time correlation dimension D_t and its local slope d_t as:

$$d_t(r,\tau) = \frac{\partial \log C_c(r,\tau)}{\partial \log \tau},\ D_t(\tau) = \lim_{\tau \to 0} d_t(r,\tau),$$

and the space correlation dimension D_s with its local slope d_s as:

$$d_s(r,\tau) = \frac{\partial \log C_c(r,\tau)}{\partial \log r},\ D_s(r) = \lim_{r \to 0} d_s(r,\tau).$$

The results show a statistical property of the different seismic catalogues that can be interpreted as an average behavior of seismic events following each earthquake.
Figure 2 shows the local slope of time correlation dimension for all considered catalogues. The overall pattern is quite similar for all catalogues. The blue domain, corresponding to low d_t values,

identifies time clustering. This means that, after the occurrence of each event, there is a space-time domain inside which the subsequent events, probably belonging to the seismic sequence, have temporally clustered occurrences. The blue domain has the greatest spatial extension at 10 days for the global catalogue, while for regional one it reaches its maximum at around one month. During the days after this time, the clustering domain spatially shrinks, but it is still present after more than 8 years (less for global CMT catalogue). Orange and red colors identify a relatively high time correlation dimension. At distances and time interval corresponding to this domain, the earthquakes occurrence approaches a random process, denoting the disappearance of the sequence or the overlapping of a sufficient number of independent sequences. This happens for large distances and long time intervals as expected, but even shortly after the reference earthquake (less than 10 days).
Comparing the analyzed catalogues, we note the different extension of the clustering domain, reaching distances ranging at its maximum 130 km (for Italy) to 500 km (for global catalogue). To test the effect of different magnitude threshold we cut the Italian catalogue minimum magnitude to respectively 2, 2.5, 3, 3.5. The comparison of time correlation dimension is shown in figure 3. From the figure it is evident how the clustering domain reaches longer distances as magnitude threshold increases, even if this effect is partially blurred by the increase of noise, due to the reduced number of data. On the other hand, catalogues of Greece and Japan were analyzed with the same threshold (m=4.5); catalogues of California and Italy have the threshold at m=2.5. For this reason the explanation of the difference between members of each couple (sharing the same magnitude threshold) could be linked to the strongest earthquake recorded in each catalogue, that is: m=9.5 for global CMT, m=7.5 for Greece, m=8.3 for Japan, m=7.3 for South California and m=5.8 for Italy.
Concerning the space correlation dimension d_s (figure 4), results reveal in each catalogue the presence of a space clustering of hypocenters for distances greater than few tenth of *km* and for time intervals less than hundreds of days. For longer time intervals, the disappearance of spatial clustering reveals the seismic structures related to preexisting tectonic settings, such as plate boundaries for bigger scales examples; after a sufficiently long time evolution, seismicity will tend to fill these seismic structures up to dimensions of thousands of kilometers. At short distances, d_s values mark clearly the presence of a zone, around each source, where hypocenters are not space clustered, but they tend to fill the space. The pairs of events, belonging to this domain, are characterized by time clustering, as showed before, for time intervals longer than 10 days. There is no clear demarcation of this near-source domain, but when fixing the limit of clustering at as example $d_s = 1.5$, it appears that the area with high correlation dimension is evolving with time. The separation line defines a radius, slowly growing in time, within which seismic events are spatially more uniformly distributed. This finding is in agreement with the accepted migration of aftershocks away from a main shock (Tosi et al., 2008).
Even in this case the overall pattern is very similar for the various catalogues, but the mean extension of the near source domain varies from 8 km (California and Italy), 16 (Greece and Japan) to 40 km (global CMT). Is Interesting to note that the analysis of Italian catalogue at increasing magnitude threshold (figure 5) do not produce significant differences in the pattern. Only the increase of noise is evident. Even maximum earthquake magnitude does not seem to drive d_s pattern. Probably the variation of the near-source extension is due to tectonic setting, as Japanese, Greek and global seismicity are dominated by big trust earthquakes, whereas Italian and Californian have more direct and strike-slip faults.

Omori law analysis

This analysis is focused on time decay of seismic activity. Traditionally this analysis is dedicated to the study of seismic sequence produced by a main shock (Omori, 1894). Later Utsu (1961) defined the empirical so called modified Omori law (MOL):

$$n(t) = \frac{k}{(c+t)^p}.$$

Where $n(t)$ is the number of earthquakes per day, t is time from the main shock, k reflects the seismic productivity and c is the "time offset" parameter; p modifies the decay rate and typically falls in the range 0.7–1.5.

The common approach is to take a big event as a main shock. After having defined a suitable area, comprising generally the seismogenic fault, all related events following the main shock are grouped inside a proper time unit (generally one day) and counted.

We are interested to analyze space-time relations of earthquakes triggered by a main event. Assuming that every event can be a main shock of its own sequence, we count all succeeding events in function of both time and space distances. This space-time count is repeated for all N events and the result is a stacked generalized count:

$$n(r,\tau) = \frac{1}{NS\Delta\tau} \cdot \sum_{i=1}^{N-1} \sum_{j=i+1}^{N} \left(\Theta(R_1)\cdot\Theta(R_2)\cdot\Theta(\mathrm{T}_1)\cdot\Theta(\mathrm{T}_2)\right),$$

where r and τ represents, respectively, space and time distances from parent events. S is the area normalization coefficient:

$$S = \pi\left(\left(r+\frac{\Delta r}{2}\right)^2 - \left(r-\frac{\Delta r}{2}\right)^2\right),$$

Δr and $\Delta\tau$ represent the size of respectively space and time windows for the events counting. R_1, R_2, T_1 and T_2 are respectively:

$$R_1 = \left(r+\frac{\Delta r}{2}\right) - \left\|\mathbf{x}_i - \mathbf{x}_j\right\|,$$

$$R_2 = \left\|\mathbf{x}_i - \mathbf{x}_j\right\| - \left(r-\frac{\Delta r}{2}\right),$$

$$\mathrm{T}_1 = \left(\tau+\frac{\Delta\tau}{2}\right) - \left\|t_i - t_j\right\|,$$

$$\mathrm{T}_2 = \left\|t_i - t_j\right\| - \left(\tau-\frac{\Delta\tau}{2}\right)$$

and Θ is the Heaviside step function.

It is worth to note that, taking into account different spatial distances, the number of event pairs at bigger distances is simply increased according to the geometrical expansion of the area embedding the events. To account this effect the number of succeeding events is given normalized by the area of the circular annulus at a given distance.

The result of the Omori count is given at three distance ranges, same for all analyzed catalogues. Specifically these ranges are: 3-10km, 10-32km and 32-100km. In figure 6 they are displayed respectively in blue (closest range), green (intermediate) and red (farthest) for all five catalogues.

As expected the closest range shows a quite similar behavior to the standard Omori count, as made from a single main event. This feature has two specific meanings: a) the standard Omori count reflects the number of events decay at small distances from the epicenter, as defined by the size of the seismic fault; b) the stacked generalized count is in agreement with the standard Omori law in terms of c and p parameters.

The behaviour of the stacked Omori counts, for each catalogue, can be influenced by specific factors like: number of events, range of magnitudes present into the catalogue (defined as $m_{max} - m_{min}$), minimum magnitude of catalogue, tectonic settings of seismic area.

We can note common features in all five catalogues.

- A first part (times from parent shock occurrence until 1-10 days) in which the decay rate is very low. This feature is usually modelled with the presence of the *c* constant into the MOL. California catalogue shows it in the clearest fashion. This is due to the very low minimum completeness magnitude limit, reflected by the highest number of events per unit area (slightly less than 10^{-1} events/km^2 for the closest range). This first portion is present in all catalogues for all distance ranges (sole exception is represented by 32-100km range (red) for the Italian catalogue).
- A medium part of power law decay typical of the Omori law and represented by the exponent *p*. Time validity of this behavior is from 1 to 100 days for world, and Greek catalogues; from 1 to 300 days for Californian, Italian and Japanese catalogues. Values of p constant are into the interval $0.87 < p < 1.36$ for closest range, $0.76 < p < 1.12$ for intermediate range and $0.24 < p < 0.68$ for longest distant range.
- A last part where decay is very low and normalized number of events is the lowest and quite similar for all three spatial ranges.
- The behavior of two spatial ranges closest to the main shock is similar, while the farthest range is quite different: this feature applies to all five catalogues.

Spatial ranges discrimination of Omori analysis gives a further element to establish the length of a sequence: in fact a sequence lasts until a decay rate of events is present. Moreover we can assume that a sequence lasts until there is a marked difference of number of events per unit area at different distance ranges. This is due to the fact that the presence of aftershocks is higher close to the mainshock. In all five analyzed catalogues we can note that the difference of number of events per unit area is biggest at times closest to main shock occurrence, and this difference tends to reduce in time. In fact aftershocks are more concentrated near and at closest times to the main shock. In time, the Omori law behavior appears to be linked to spatial distances from the main shock and it is followed by a change of rate right before the end of the sequence.

An interesting result comes out from the comparison with the analysis of temporal fractal dimension as function of space and time. The temporal clustering caused by an event lasts for longer time in respect to the end of the Omori power law (see figure 2). This suggests a different definition of a seismic sequence, in dependence of the analyzed aspects: time, space and occurrence rate. In fact, while the rate decay pertains to the seismic activity increase due to sequence triggering, the temporal clustering takes account of occurrences disposition in the time axis. Low time fractal dimension indicates time clustering of events. When the seismic sequence is characterized by an increased seismic activity, it is easily recognizable. On the other side, time clustering in periods of normal or slightly high background activity may indicate that the influence of the mainshock is still present. This influence probably reflects the persisting of triggering by parent events: the seismic activity, although at background rates, is not random, as it is still driven by main-aftershocks relations embedded inside background activity. Time clustering is due to clusters of events and voids caused by seismic shadows, as frequently observed at long timescales (Marsan, 2006).

Conclusions

Seismic sequences have been traditionally defined, in relation with the main shock, hence enclosing the succeeding events at limited spatial ranges. In general all events located in the seismic main fault have been considered related to the main shock. Such definition allowed the early discovery of the decay law by Omori (Omori 1894, Utsu 1961), which is a simple and interesting statistical definition of a sequence. In this work we have proposed an extension of the definition of a sequence by the introduction of space-time constrains for the analysis of decay rate and clustering. To allow such space-time analysis we have operated a stacking procedure: it consisted in considering every event as a mainshock and merging all subsequent seismic events in a stacked sequence. Davis and Frohlich (1991) with Nyffenegger and Frohlich (1998) already applied the stacking approach. We

have used and analyzed five different seismic catalogues characterized by various space and magnitude ranges, spanning from a global catalogue to regional ones.
Stacked approach, in the constitution and analysis of sequences, allowed a more stable statistical analysis, as required by the added spatial distinction. Results are in agreement with the standard Omori *p* values but more articulated. In fact the slope of the decay rate is small in the first time period after the main shock (first 10-20 days) before to reach typical Omori values. Behavior is influenced by spatial distance: *p* values are smaller when the distance from parent shock increases. After a period of hundreds of days the typical Omori *p* values disappear in favor of little or not decay. This happens in conjunction with the disappearing of differences in function of distance. We interpret this as a closing of the typical sequence period.
Space-time fractal dimension analysis was analyzed as mean behavior, maintaining the same approach of stacking. After the occurrence of an event there is, for all investigated catalogues, a space-time domain inside which earthquakes are time clustered, denoting close relationships among events. Strong space clustering is present but only at distances bigger than seismic faults size, otherwise space fractal dimension is around 1.5 in agreement with fault fractal dimension. The time clustering domain denotes that in a particular space-time range after the occurrence of a seismic events, earthquakes are not random.
Interestingly sequences maintain time clustering longer than the sequence end indicated by the stacked Omori law result. Time clustering evidences that the influence of the parent shock is still present even if seismicity is at background rate. This method could thus be used to detect seismic shadows after the end of the sequence.
The space-time analysis of seismic sequences, allowed by stacking of seismicity and considering every event as mainshock, shows a more detailed analysis of seismicity under triggering effects: results are in agreement with standard analysis of sequences and add a deeper insight to the topic. Influence area of seismic activity, related to a mainshock, is dynamically sized, giving further constrains to sequence modeling.

Acknowledgements

The study was supported by INTAS Project Nr: 05-1000008-7889, by EU FP6 NEST Pathfinder programme TRIGS under contract NEST-2005-PATH-COM-043386 and by the DPC (Dipartimento della Protezione Civile) S1 2007-2009 Project.

References

Bak, P. & Tang C., 1989. Earthquakes as a self-organized critical phenomenon, J. Geophys. Res., 94, 15635-15637.

Brodsky, E. E., Karakostas, V. & Kanamori, H., 2000. A new observation of dynamically triggered regional seismicity: earthquakes in Greece following the August, 1999 Izmit, Turkey earthquake, Geophys. Res. Lett., 27, 2741–2744.

Davis S.C. & Frohlich C., 1991. Single-Link Cluster Analysis of Earthquake Aftershocks: Decay Laws and Regional Variations, J. Geophys. Res., 96, 6335-6350.

Gasperini, P. & Mulargia, F., 1989. A statistical analysis of seismicity in Italy: The clustering properties, Bull. Seismol. Soc. Am., 79, 973-988.

Godano, C., Tosi, P., De Rubeis, V. & Augliera, P., 1999. Scaling properties of the spatio-temporal distribution of earthquakes: a multifractal approach applied to a Californian catalogue, Geophys. J. Int., 136, 99-108.

Hill, D.P., Reasenberg, P.A., Michael, A., Arabaz, W.J., Beroza, G., Brumbaugh, D., Brune, J.N., Castro, R., Davis, S., dePolo, D., Ellsworth, W.L., Gomberg, J., Harmsen, S., House, L., Jackson, S.M., Johnston, M.J.S., Jones, L., Keller, R., Malone, S., Muaguia, L., Nava, S., Pechmaann, J.C., Sanford, A., Simpson, R.W., Smith, R.B., Stark, M., Stickney, M., Vidal, A., Walter, S., Wong, V. & Zollweg, J., 1993. Seismicity remotely triggered by the magnitude 7.3 Landers, California, earthquake, Science, 260, 1617-1623.

Husen, S., Wiemer, S. & Smith, R.B., 2004. Remotely Triggered Seismicity in the Yellowstone National Park Region by the 2002 Mw 7.9 Denali Fault Earthquake, Alaska, Bull. Seismol. Soc. Am., 94, 6B, 317-331.

King, G.C.P., Stein, R.S. & Lin, J., 1994. Static stress changes and the triggering of earthquakes, Bull. Seismol. Soc. Am., 84, 935-953.

Lomnitz, C., 1996. Search of a worldwide catalog for earthquakes triggered at intermediate distances, Bull. Seismol. Soc. Am., 86, 293-298.

Marsan, D., Bean, C.J., Steacy, S. & McCloskey, J., 2000. Observation of diffusion processes in earthquake populations and implications for the predictability of seismicity systems, J. Geophys. Res., 105, 28081-28094.

Marsan, D:, 2006. Can coseismic stress variability suppress seismicity shadows? Insights from a rate-and-state friction model, Jou. Geoph. Res., 111, B06305.

Marzocchi, W., Selva, J., Piersanti, A. & Boschi, E., 2003. On the long-term interaction among earthquakes: Some insight from a model simulation, J. Geophys. Res., 108, 2538-2550.

Melini, D., Casarotti, E., Piersanti, A. & Boschi, E., 2002. New insights on long distance fault interaction, Earth and Planetary Science Letters, 204, 363-372.
Omori, F., 1894. On the after-shocks of earthquakes, J. Coll. Sci., Imp. Univ. Tokyo 7 (1894), 111–200.

Nyffenegger, P & Frohlich, C, 1998. Recommendations for Determining p Values for Aftershock Sequences and Catalogs, Bull. Seismol. Soc. Am., 88, 1144-1154.

Ogata, Y., L. M. Jones, and S. Toda, 2003. When and where the aftershock activity was depressed: Contrasting decay patterns of the proximate large earthquakes in southern California, J. Geophys. Res., 108(B6), 2318.

Omori, F. 1894. On the aftershocks of earthquakes, Journal of the College of Science, Imperial University of Tokyo, vol. 7, 111–200.

Reasenberg, P.A., 1999. Foreshock occurrence before large earthquakes, J. Geophys. Res., 104, 4755-4768.

Shearer, P., E. Hauksson, and G. Lin, 2005. Southern California hypocenter relocation with waveform cross-correlation, Part 2: Results using source-specific station terms and cluster analysis, Bull. Seismol. Soc. Am. 95, 904-915.

Stein, R. S., King, G.C.P. & Lin, J., 1994. Stress triggering of the 1994 M = 6.7 Northridge, California, earthquake by its predecessors, Science, 265, 1432-1435.

Stein, R. S., 1999. The role of stress transfer in earthquake occurrence, Nature, 402, 605-609.
Stein, R. S., King, G.C.P. & Lin, J., 1994. Stress triggering of the 1994 M = 6.7 Northridge, California, earthquake by its predecessors, Science, 265, 1432-1435.

Tosi, P., De Rubeis, V., Loreto, V. & Pietronero, L., 2008. Space–time correlation of earthquakes Geoph. Jou. Int. 173,3,932-941.

Utsu T., 1961. A statistical study on the occurrence of aftershocks, Geophys. Mag. 30 (1961), 521–605.

Ziv, A., 2006. What Controls the Spatial Distribution of Remote Aftershocks?, Bull. Seismol. Soc. Am., 96, 6, 2231-2241.

Figures and figures captions

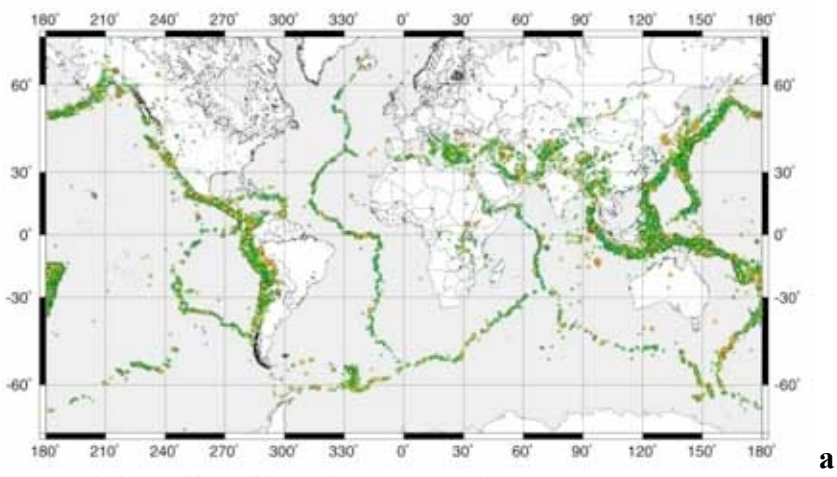

a

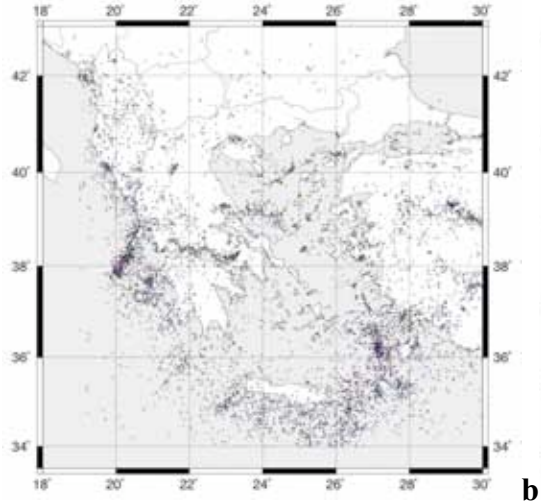

b

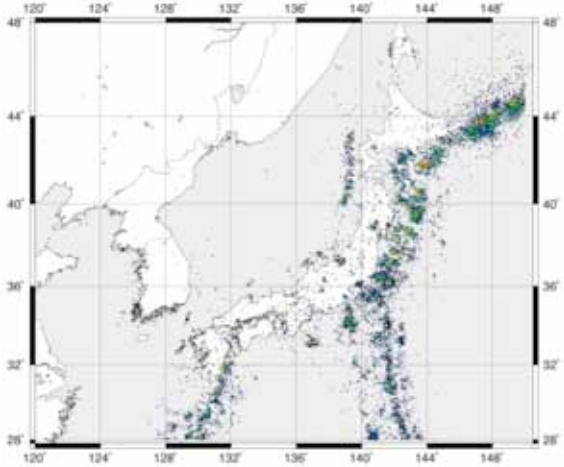

c

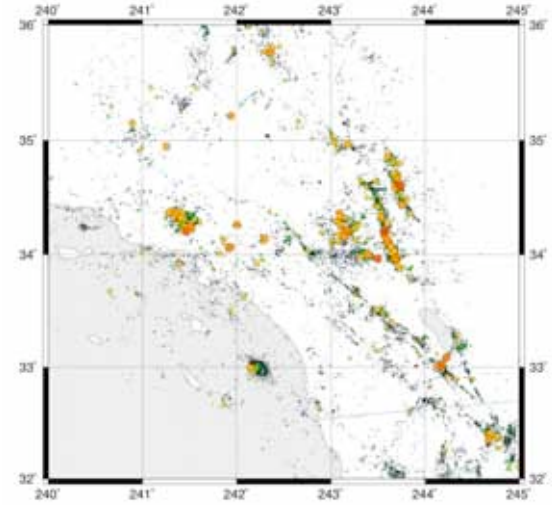

d

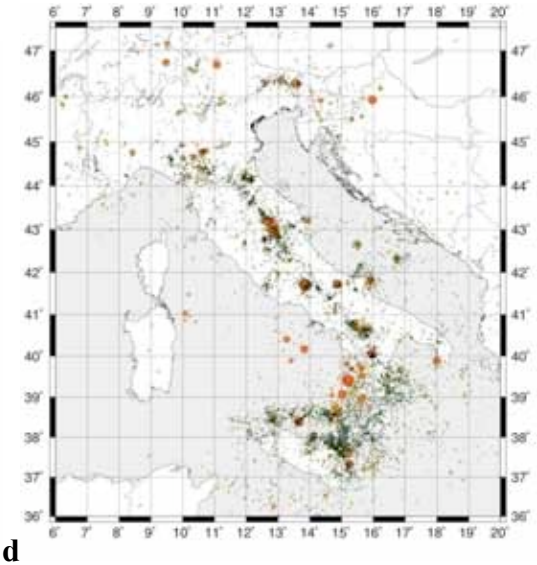

e

Figure 1. Seismic catalogues used to analyze earthquake data. They are respectively:
a) Global CMT (Centroid Moment Tensor, Harvard). January 1980 - December 2004, 13268 events. b) Greece (Geophysical Laboratory, University of Thessaloniki). January 1964 - September 2007, 5865 events. c) Japan (selection of USGS NEIC catalogue). January 1980 - October 2008, 6698 events. d) South California (Southern California Earthquake Center, relocated by Shearer et al., 2005 January 1984 - December 2002, 23576 events. e) Italy (INGV CSI 1981-2002 and ISIDE 2002-2009), January 1988 - May 2009, 11860 events.

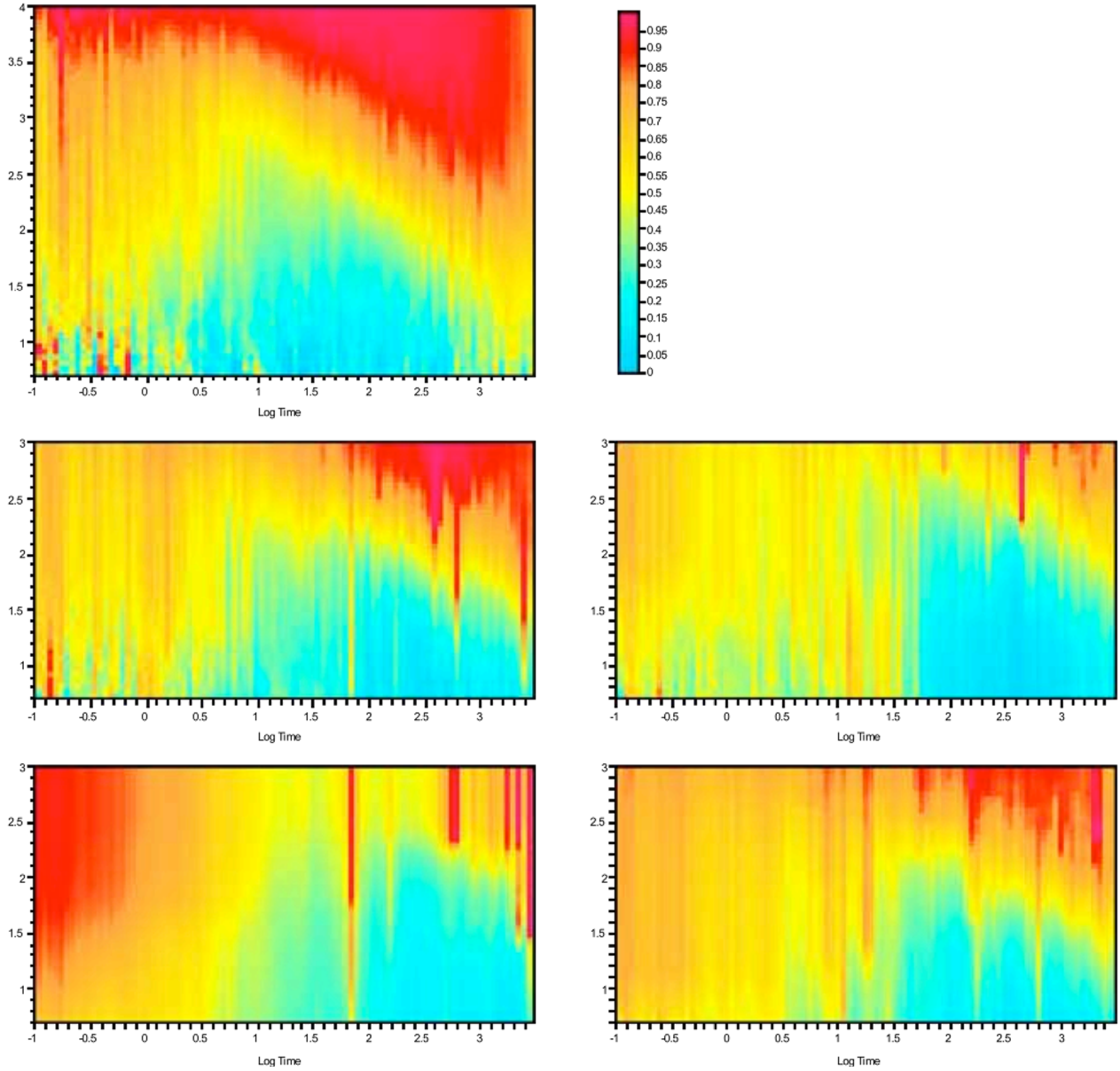

Figure 2. Local slope d_t of time correlation dimension D_t for all considered catalogues (catalogues correspond to the same position as figure 1). Time correlation dimension ranges from 0 (blue) to 1 (red) as indicated on the graduated bar.

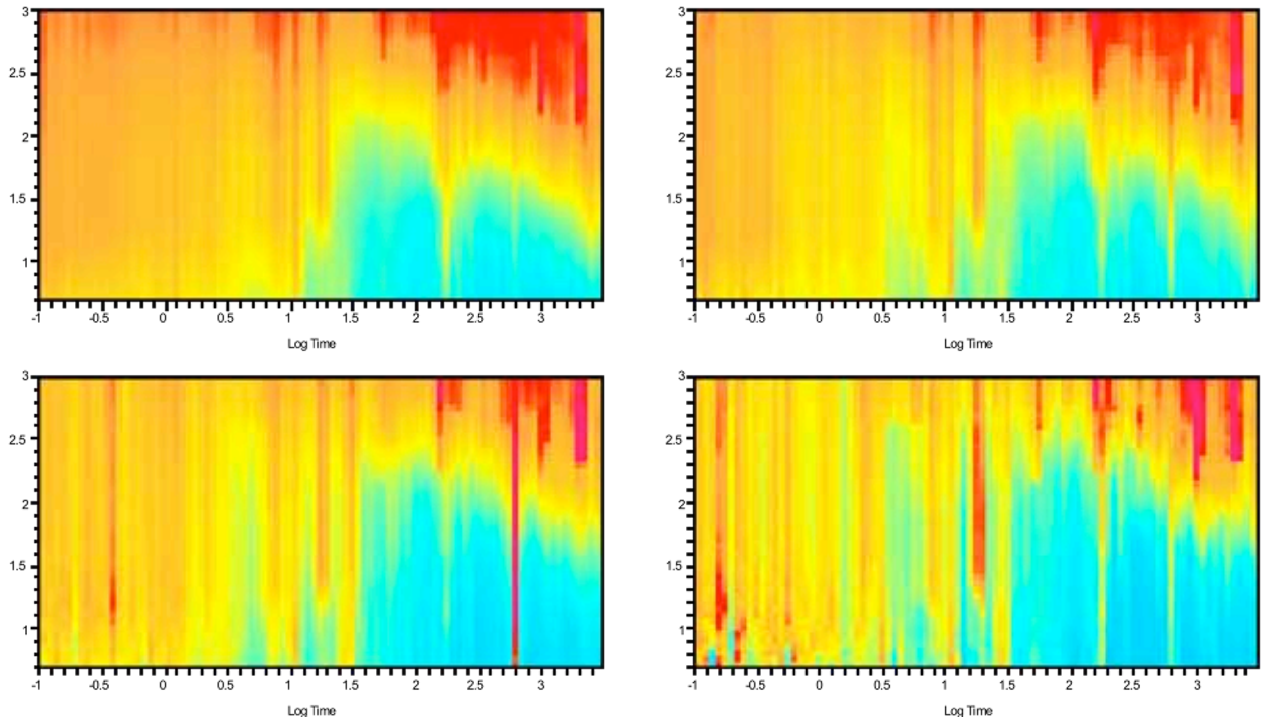

Figure 3. Effects of different magnitudes threshold in local slope d_t of time fractal dimension for the Italian catalogue. Minimum magnitudes are respectively (from top left to down right, as reading succession) $m > 2.0$, $m > 2.5$, $m > 3.0$, and $m > 3.5$.

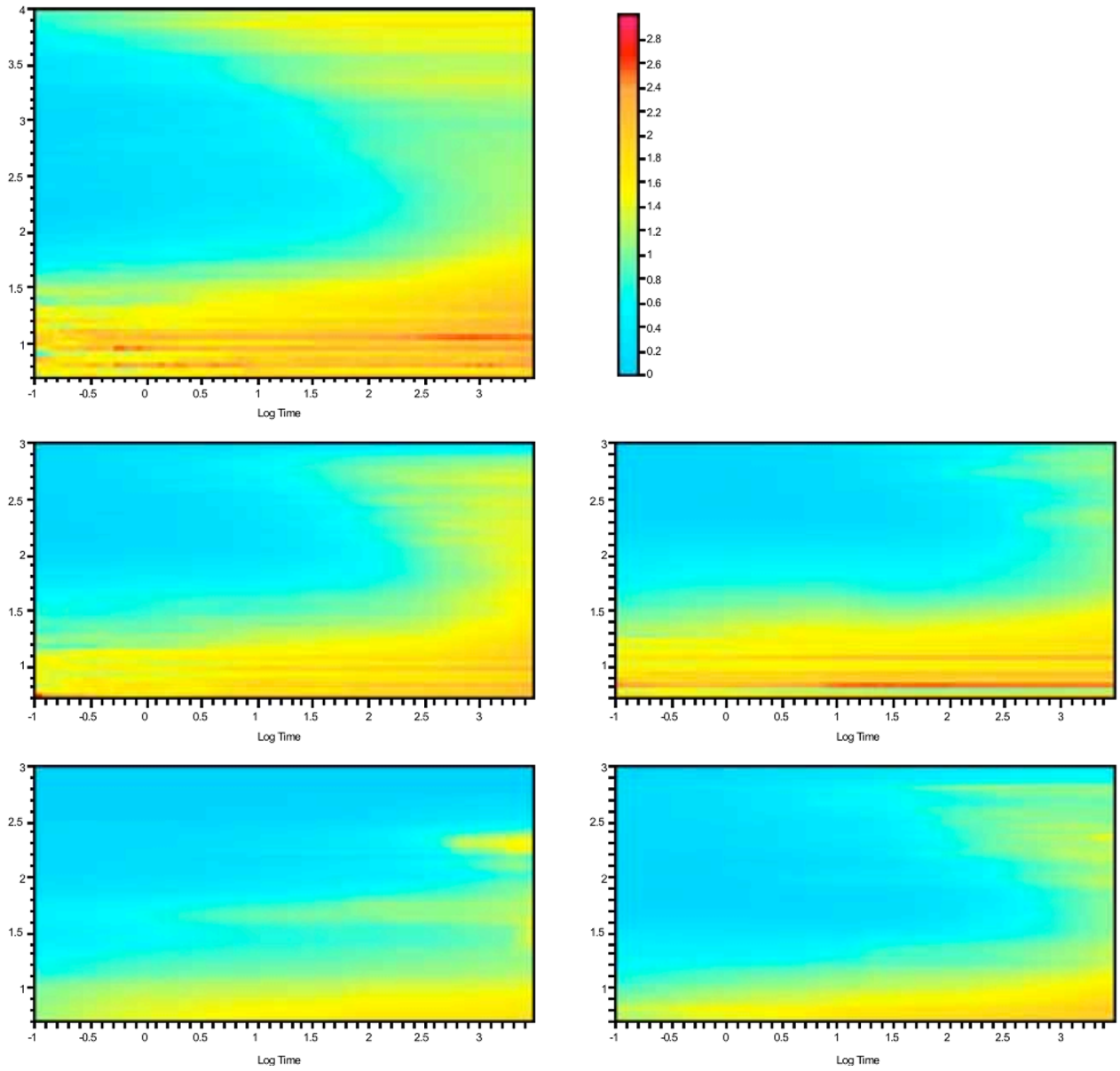

Figure 4. Local slope d_s of space correlation dimension D_s for all considered catalogues (catalogues correspond to the same position as figure 1). Space correlation dimension ranges from 0 (blue) to 3 (red) as indicated on the graduated bar.

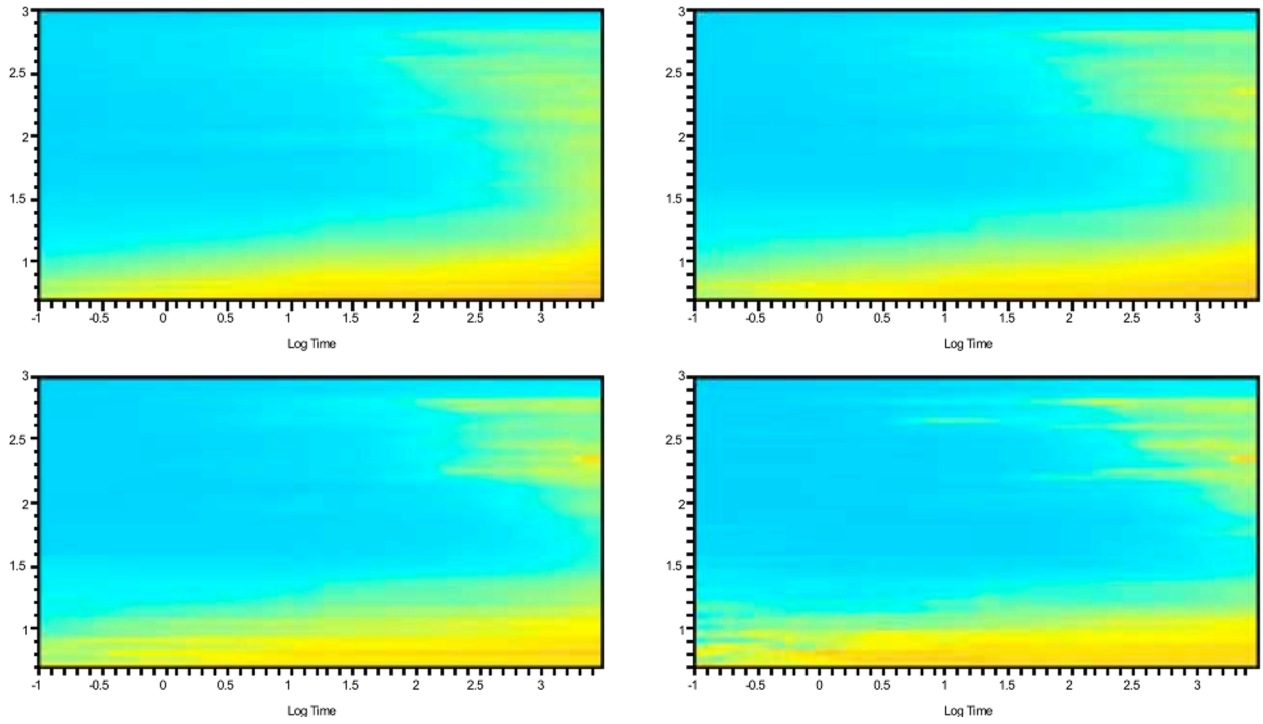

Figure 5. Effects of different magnitudes threshold in local slope d_s of space fractal dimension for the Italian catalogue. Minimum magnitudes are respectively (from top left to down right, as reading succession) $m > 2.0$, $m > 2.5$, $m > 3.0$, and $m > 3.5$.

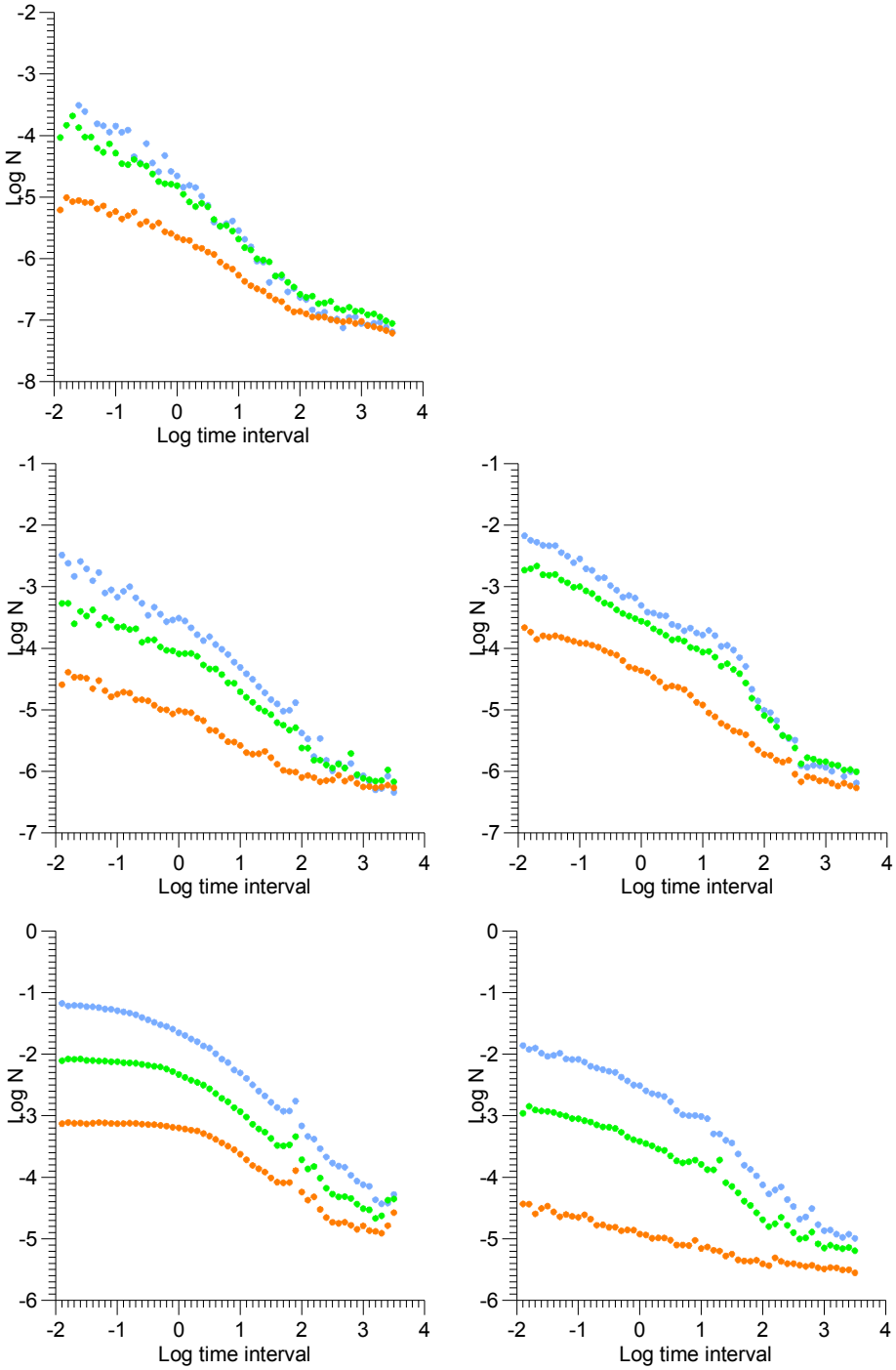

Figure 6. Log-Log plot of the number of events for time (day) and space (km^2) unit (stacked Omori count) at three distance ranges, for all analyzed catalogues (refer to figure 1). Distance ranges are: 3-10km (blue), 10-32km (green) and 32-100km (red).